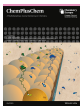

Europium(III) Macrocyclic Chelates Appended with Tyrosine-based Chromophores and Di-(2-picolyl)amine-based Receptors: Turn-On Luminescent Chemosensors Selective to Zinc(II) Ions

Gaoji Wang,[a] Carlos Platas-Iglesias,[b] and Goran Angelovski*[a]

Zinc ions play an important role in many biological processes in the human body. To selectively detect Zn^{2+}, two EuDO3A-based complexes (DO3A = 1,4,7,10-tetraazacyclododecane-1,4,7-tricarboxylic acid) appended with tyrosine as a chromophore and di-(2-picolyl)amine (DPA) as the Zn^{2+} recognition moiety were developed as suitable luminescent sensors. Their luminescence intensity is affected by the photoinduced electron transfer mechanism. Upon addition of Zn^{2+}, both probes display an up to sevenfold enhancement in Eu^{3+} emission. Competition experiments demonstrated their specificity toward Zn^{2+} over other metal ions, while also revealing the nonspecificity of the derivatives lacking the DPA-moiety, thus confirming the essential role of the DPA for the recognition of Zn^{2+}. The induced emission changes of Eu^{3+} allow for precise quantitative analysis of Zn^{2+}, establishing these lanthanide-based complexes as viable chemosensors for biological applications.

Introduction

Zinc ions are the second most abundant transition metal ions in the human body. They play a fundamental role in living systems as they are involved in many essential biological processes, including enzyme activity, signaling and gene transcription.[1] In vivo, Zn^{2+} is present in the free and protein-bound form. The abundance of Zn^{2+} is particularly important in the brain, breast, prostate and pancreas.[2] While it is not redox active under physiological conditions, Zn^{2+} deficiency is known to cause increased oxidative stress contributing to the development of different pathologies, such as cancer.[3] Therefore, its concentration in healthy organs is highly regulated by the cells through transporters and metallochaperones.[1c] Thus, imaging Zn^{2+} by non-invasive techniques is of paramount importance to understand its biological role and improve early-stage disease detection.[1c]

Due to low cost and high instrument sensitivity, a large number of optical probes and related toolboxes have been developed for the detection of Zn^{2+} in the last few decades.[1d,4] One of the commonly used chelators for sensing of Zn^{2+} is di-(2-picolyl)amine (DPA),[5] which is known to form stable complexes with Zn^{2+}, providing the molecular recognition complexes known as Zn-DPA.[6] Furthermore, combining the Zn-DPA moiety with a luminescent center can result in Zn^{2+}-responsive optical imaging probes. In 2009, the Zn^{2+} sensor Zinpyr-1 was synthesized and studied by Lippard and co-workers.[7] Zinpyr-1, bearing the DPA moiety, can respond to Zn^{2+} coordination through fluorescence quenching by photo-induced electron transfer (PET)[8] occurring in the absence of Zn^{2+}. The presence of Zn^{2+} results in an enhancement in the fluorescence emission intensity. The three nitrogen atoms of DPA strongly coordinate Zn^{2+}, with a dissociation constant (K_d) in water media of around 10^{-10} M, giving rise to the 'turn-on' fluorescence response of Zinpyr-1.[7] However, this probe also presents some disadvantages such as a small Stokes shift, low water solubility, short lifetime and broad spectra of the emission, limiting its application as an organic fluorescein compound.[1a,6d]

Due to larger Stokes shifts (> 200 nm), a longer emission lifetime in the order of milliseconds and a higher water solubility compared to the typical organic fluorescence compounds, the complexes of lanthanide trivalent ions (Ln^{3+}) such as Eu^{3+} or Tb^{3+} have been employed as Zn^{2+}-selective sensors.[4b,9] In 2004, Nagano and coworkers developed a Eu^{3+}-based chemosensor appending a DPA arm for Zn^{2+} recognition.[1a] The quinolyl moiety was applied as a chromophore to achieve a longer excitation wavelength (~320 nm). Upon addition of Zn^{2+}, the luminescence can be strongly enhanced. To efficiently coordinate the Ln^{3+} ions, DO3A (1,4,7,10-tetraazacyclododecane-1,4,7-triacetic acid) is widely and successfully used as a backbone for the development of

[a] G. Wang, Dr. G. Angelovski
MR Neuroimaging Agents,
Max Planck Institute for Biological Cybernetics,
Max-Planck-Ring 11, 72076 Tübingen (Germany)
E-mail: goran.angelovski@tuebingen.mpg.de
[b] Prof. Dr. C. Platas-Iglesias
Centro de Investigacións Científicas Avanzadas (CICA)
and Departamento de Química
Facultade de Ciencias
Universidade da Coruña
A Coruña, Galicia (Spain)

Supporting information for this article is available on the WWW under https://doi.org/10.1002/cplu.201900731

This article is part of a Special Collection on "Fluorescent Biomolecules and their Building Blocks".

© 2020 The Authors. Published by Wiley-VCH Verlag GmbH & Co. KGaA. This is an open access article under the terms of the Creative Commons Attribution License, which permits use, distribution and reproduction in any medium, provided the original work is properly cited.

© 2020 The Authors. Published by Wiley-VCH Verlag GmbH & Co. KGaA

ligands. Given the high stability of DO3A-based Ln^{3+} complexes, their properties such as luminescence and magnetic behavior have been extensively studied.[9a,b,10] However, the luminescence intensities of such LnDO3A complexes are very weak due to their inefficient direct excitation (the *f-f* transitions of the ions are Laporte-forbidden). Hence, the performance of Ln^{3+}-based luminescent probes may often be enhanced by excitation of the Ln^{3+} via a sensitizing chromophore. This moiety is included in the structure of the ligand giving the so-called chromophore-luminophore complex.[10a,11] By combining Ln^{3+} complexes and antenna moieties, the Laporte-forbidden transitions can be circumvented. The natural amino acid tyrosine (Tyr), bearing a phenol group can serve as a good antenna.[9a,12] Once it is excited by UV light, radiationless energy is transferred from tyrosine to the Ln^{3+} center, resulting in the characteristic luminescence of this metal ion.

To build upon the previous studies and prepare a potent Zn^{2+} luminescence lanthanide-based sensor, we designed, synthesized and investigated two Eu^{3+} probes, **EuL^1** and **EuL^2**, functionalized with Tyr as a chromophore and DPA as the Zn^{2+} recognition moiety (Figure 1). The Tyr unit was incorporated into the ligand designed to serve as an antenna, transferring energy efficiently to Eu^{3+}, and also as a molecular linker that connects the Eu^{3+} and Zn^{2+} chelating units. These two probes were anticipated to show an enhancement of luminescence upon Zn^{2+} addition with a long wavelength Eu^{3+}-centered emission (617 nm). Hence the large apparent Stokes shift between the excitation and emission wavelengths of the antenna and the lanthanide metal ion, respectively (~300 nm), combined with the high water-solubility typically expected for such complexes, could potentially be utilized for practical applications. Furthermore, two additional complexes **EuL^3** and **EuL^4** lacking the DPA-moiety were synthesized and utilized for comparative studies (Figure 1), expecting to highlight the effect of the Zn^{2+}-sensitive chelator on the final properties of the complexes.

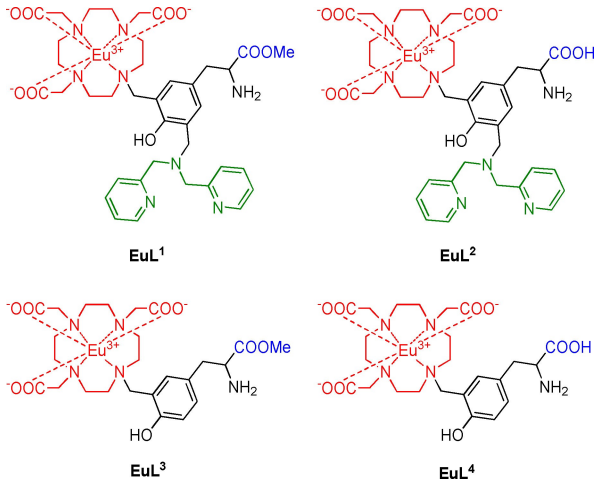

Figure 1. Chemical structures of **EuL$^{1-4}$** discussed in this work.

Results and Discussion

Design and synthesis of EuL$^{1-4}$

The probes **EuL$^{1-4}$** were synthesized in a stepwise manner, starting from the protected amino acid Boc-Tyr-OMe (Scheme 1). Firstly, DPA was coupled to Boc-Tyr-OMe to give **1** following a previously reported literature procedure.[13] Subsequently, this molecule was coupled to the DO3A moiety by reacting **1** with *t*BuDO3A in the presence of paraformaldehyde at 110 °C to afford macrocycle **2**.[14] The ligand **L^1** was obtained by treating **2** with TFA in CH_2Cl_2, followed by HPLC purification. Subsequently, basic hydrolysis of the methyl ester of **L^1** was achieved with LiOH giving **L^2** (Scheme 1a). In parallel, the ligands **L^{3,4}** were prepared directly by combining the amino acid Boc-Tyr-OMe and the *t*BuDO3A to give the macrocycle **3**

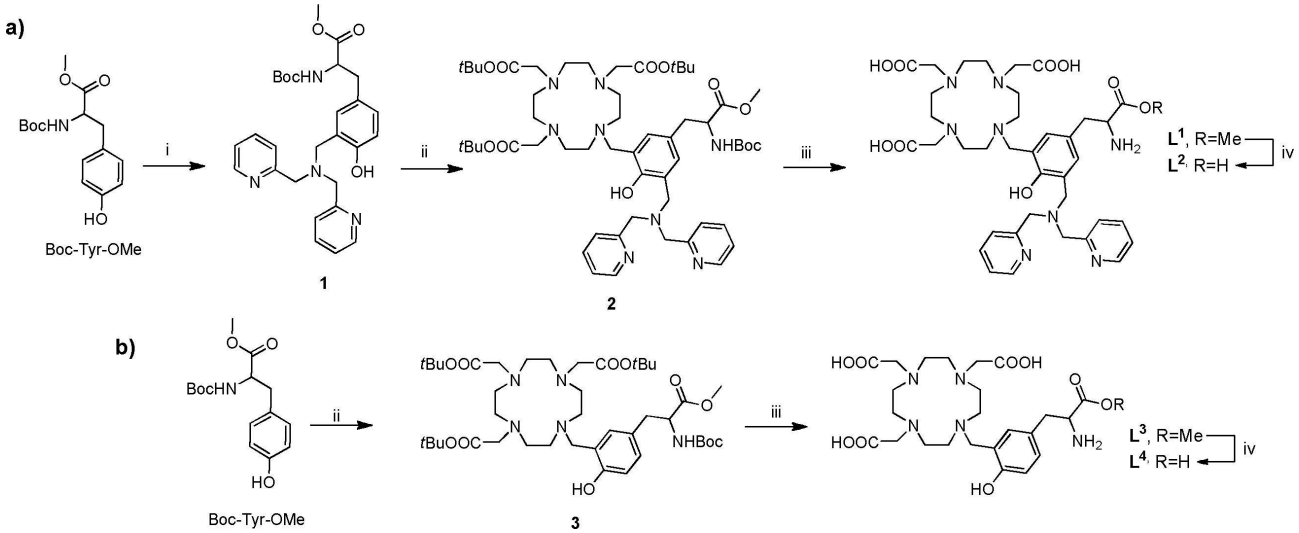

Scheme 1. The synthetic routes to ligands a) **L^{1,2}** and b) **L^{3,4}**. Reagents and conditions: i) MeOH, di-(2-picolyl)amine, $(CH_2O)_2$, 65 °C, 5 h; ii) DBU, $(CH_2O)_2$, toluene, 110 °C, 6 h for **2** and 65 °C, 3 h for **3**; iii) TFA, CH_2Cl_2, 18 h; iv) LiOH, MeOH, 18 h.

© 2020 The Authors. Published by Wiley-VCH Verlag GmbH & Co. KGaA

(Scheme 1b). Acid hydrolysis with TFA resulted in the ligand **L**^{3}, which was further subjected to basic hydrolysis with LiOH to provide the ligand **L**^{4}. Finally, all the complexes **EuL**$^{1-4}$ were prepared by treating the ligands with $EuCl_3 \cdot 6H_2O$ in water, while maintaining the pH at ~7.

Luminescence properties of EuL$^{1-4}$

Competition with biologically relevant cations

The **EuL**$^{1-4}$ complexes present weak luminescence upon excitation through the ligand bands at 322 nm (HEPES buffer, pH 7.4). Due to such weak emission, no luminescence lifetime values could be determined to evaluate the hydration number (*q*) of each complex. Instead, estimation of the hydration state of the studied complexes was based on the results obtained from the relaxometric studies of the Gd^{3+} analogues (see below).

The addition of Zn^{2+} has quite different effects on the luminescence emission intensity for these complexes. Specifically, both **EuL**^{1} and **EuL**^{2} exhibit an increase in emission intensity upon the addition of one equivalent of Zn^{2+}, while another equiv. of Zn^{2+} causes a further but smaller increase in emission for **EuL**^{1} only. Meanwhile, both **EuL**^{3,4} remain insensitive to the addition of Zn^{2+}, confirming that the presence of the DPA moiety is essential to affect the luminescence emission (Figure 2a).

The selectivity of **EuL**^{1,2} was further tested by addition of metal ions commonly found in biological systems. Chloride salts of K^+, Na^+, Ca^{2+}, Mg^{2+}, Fe^{2+} and Fe^{3+} (3 equiv.) do not provoke significant changes in the intensity of the Eu^{3+} $^5D_0 \rightarrow {}^7F_J$ transitions ($J=0$ to 4),[15] while Cu^{2+} almost completely quenches the Eu^{3+}-based luminescence. Subsequent addition of Zn^{2+} (3 equiv.) results in a dramatic enhancement of the emission intensity in the presence of K^+, Na^+, Ca^{2+}, Mg^{2+}, Fe^{2+} and Fe^{3+}, indicating the selective response of **EuL**^{1,2} to Zn^{2+} in the presence of these competing metal ions (Figures 2b and S1 in the Supporting Information). Only Cu^{2+} was found to compete efficiently with Zn^{2+} among the metal ions examined in this study. This is however expected considering the higher affinity of DPA for Cu^{2+} compared with Zn^{2+},[16] and the known ability of Cu^{2+} to quench the emission of organic chromophores due to its partially occupied 3d shell.[17] However, the luminescence quenching effect of Cu^{2+} is not likely to be a significant problem for practical applications because free copper ions in living cells are present in very low quantities.[18] As expected, **EuL**^{3,4} exhibit weak and random luminescence changes toward all of these studied ions. The high selectivity toward Zn^{2+} suggested that probes **EuL**$^{1-2}$ can be useful for potential biological applications.

Titrations with Zn^{2+}. Since **EuL**^{1} and **EuL**^{2} exhibited different responses to the addition of Zn^{2+}, we conducted more detailed studies with these two systems. Increasing amounts of Zn^{2+} were added to an aqueous solution of **EuL**^{1} (50 μM) and the steady-state emission spectra were recorded from 560 to 720 nm using the same excitation wavelength (322 nm). By

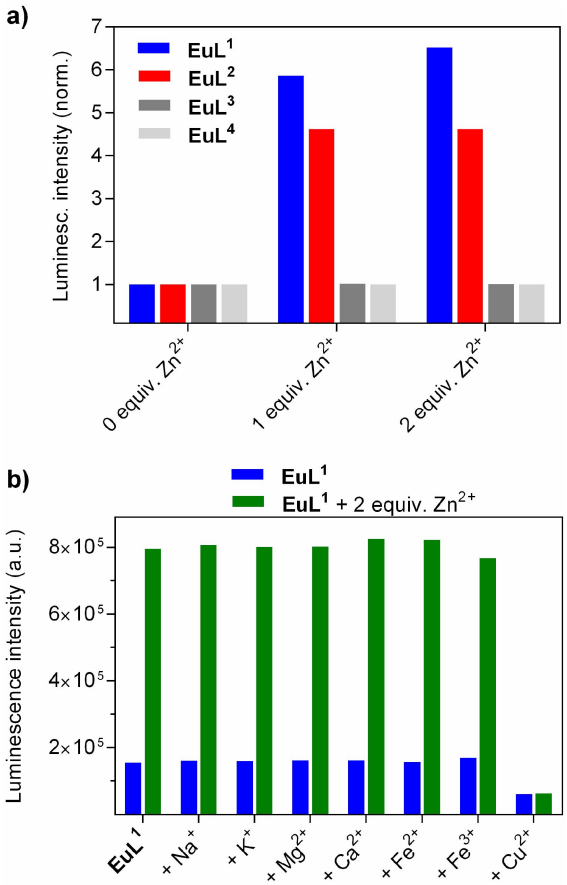

Figure 2. a) Luminescence changes of **EuL**$^{1-4}$ (50 μM) upon addition of Zn^{2+}. All data were recorded in HEPES buffer (50 mM, pH 7.4) with $\lambda_{ex}=322$ nm and $\lambda_{em}=617$ nm; intensity was estimated by the peak height at $\lambda_{em}=617$ nm. b) Luminescence variations of **EuL**^{1} (50 μM) to Zn^{2+} in the presence of different metal ions. Blue bars indicate luminescence intensity of **EuL**^{1} in the presence of various metal ions (3 equiv.). Green bars indicate luminescence intensity of **EuL**^{1} after the subsequent addition of Zn^{2+} (3 equiv.).

following the most intense $^5D_0 \rightarrow {}^7F_2$ transition, the titration profile presents two inflection points close to 1:1 and ~1:2 (Eu^{3+}:Zn^{2+}) stoichiometry ratios, reaching a plateau with further Zn^{2+} addition of up to 4 equiv. (Figure 3). The emission intensity of **EuL**^{1} increased significantly (about 7-fold at 617 nm) upon the addition of two equiv. of Zn^{2+}, with a large apparent Stokes shift (295 nm). These results indicate the presence of two different Zn^{2+} binding sites: the initial increase of luminescence intensity should be ascribed to the complexation between DPA and Zn^{2+}, while the second should be related to the weak interaction between the amino acid methyl ester of tyrosine and Zn^{2+} (Figure 3 inset). The emission spectra of **EuL**^{1} were analyzed to a model including the formation of both 1:1 and 1:2 (Eu^{3+}:Zn^{2+}) species, affording association constants of $\log K_{11}=7.15\pm0.03$ and $\log K_{12}=4.59\pm0.02$ (Figure S2 in the Supporting Information). Obviously, the binding of the first equivalent of Zn^{2+} is very strong, while the second binding process is weaker. The first association constant is virtually identical to that determined for $[Zn(DPA)]^{2+}$ at pH 7.0 ($\log K_{11}=7.15$).[19]

© 2020 The Authors. Published by Wiley-VCH Verlag GmbH & Co. KGaA

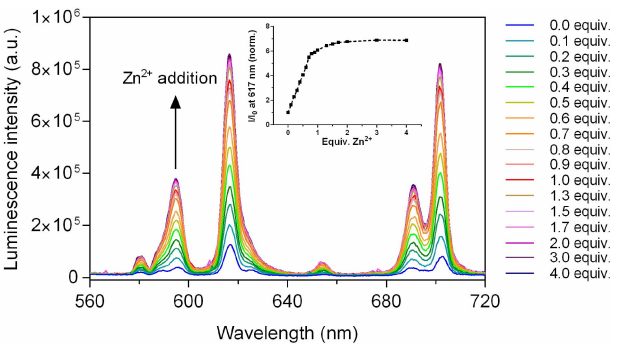

Figure 3. Luminescence emission spectral variations of **EuL^1** (50 μM, $\lambda_{ex}=322$ nm, $\lambda_{em}=617$ nm) upon titration with Zn^{2+} (50 mM HEPES, pH 7.4, 25 °C). Inset: normalized emission intensities of **EuL^1** as a function of Zn^{2+} concentration.

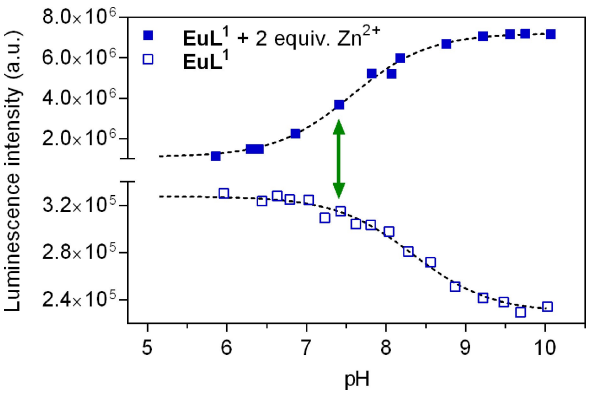

Figure 4. Luminescence emission intensity variations with pH changes of **EuL^1** (open symbols) and **EuL^{1}Zn** (filled symbols) in water (50 μM complex, 100 mM KCl as the electrolyte, $\lambda_{ex}=322$ nm; intensity was estimated by the peak height at $\lambda_{em}=617$ nm). The dashed lines represent fitted values as described in the Experimental section, while the green arrow shows the luminescence emission change at pH 7.4.

Further insights into the behavior of these systems were obtained by repeating the titration experiments with **EuL^2**, which bears a carboxylic acid on the Tyr moiety instead of a methyl ester group as in **EuL^1** (Figure S3 in the Supporting Information). The luminescence changes were investigated upon addition of Zn^{2+} within the same concentration range (0–4 equiv.). Here, the emission intensity increases 5-fold and only up to the addition of one equiv. of Zn^{2+}. The analysis of the data according to a 1:1 binding model resulted in an association constant with a value of $\log K_{11}=7.1\pm0.1$, indicating strong binding of Zn^{2+} to the DPA-tyrosine moiety (Figure S2 in the Supporting Information). We hypothesize that the amino acid of **EuL^2** exists as a zwitterion at physiological pH,[20] which consequently induces the observed luminescence increase with only one equiv. of Zn^{2+}. The situation is slightly different in **EuL^1**, where the DPA-tyrosine moiety dominates the turn-on response of luminescence; however, the positively charged Tyr moiety in the form of a methyl ester interacts with the second equiv. of Zn^{2+}, thus further promoting the luminescence emission.

Luminescence pH titrations

The pH dependence of the emission intensity of **EuL^1** and **EuL^{1}Zn** was investigated to shed light into the mechanism responsible for the turn-on response to Zn^{2+} (Figure 4). For **EuL^1**, in the absence of Zn^{2+}, the luminescence is gradually quenched by increasing pH. This is a result of photoinduced electron transfer (PET) caused by the lone pair of electrons from the DPA moiety.[21] Protonation of the amine nitrogen atom of the DPA moiety decreases the energy of the nitrogen lone pair, thus preventing the PET process. The fitting of the pH titration profile provides a pK_a of 8.3 ± 0.1, indicating that the DPA group is largely protonated under physiological conditions.

For **EuL^{1}Zn** (**EuL^1** with 2 equiv. Zn^{2+}), the luminescence is gradually enhanced with increasing pH, providing a pK_a of 7.6 ± 0.1. The relatively high equilibrium constant determined for the association of **EuL^1** with Zn^{2+} (see above) indicates that nearly all Zn^{2+} present in solution is already bound to the DPA moiety at pH 7.4. Subsequently, the pH dependent changes in luminescence emission observed for **EuL^{1}Zn** should be ascribed to a protonation process that does not involve the DPA moiety, but is likely related to the protonation/deprotonation of the phenol unit. This pK_a is considerably lower than that determined in the absence of Zn^{2+} (p$K_a=9.4\pm0.5$, see below), which opens the question of whether the phenol group remains coordinated to the lanthanide ion upon protonation. Indeed, Sherry et al. showed that a GdDO3A derivative containing a methylene nitrophenol pendant arm provided a relaxivity response to pH, as protonation of the phenol group provokes its dissociation from the lanthanide center, resulting in an increase of the number of coordinated water molecules.[22]

Similarly to **EuL^1**, the **EuL^2** and **EuL^{2}Zn** complexes show similar pH titration profiles (Figure S4 in the Supporting Information). Here, the pK_a values are almost identical to those of the **EuL^1**/**EuL^{1}Zn** pair, resulting in values of 8.2 ± 0.1 and 7.5 ± 0.1 for **EuL^2** and **EuL^{2}Zn**, respectively. This provides additional evidence that the pK_a observed for the **EuL^{1}Zn** complex can be associated to the protonation of the phenol group from the Tyr moiety. Indeed, the similar pK_a values of the **EuL^{1,2}**/**EuL^{1,2}Zn** systems suggest that both groups experiencing protonation (amine and phenol groups of the DPA and phenol moieties, respectively) are not affected significantly by the different functional groups of the amino acid part of Tyr, i.e. the ester and free acid in **EuL^1** and **EuL^2**, respectively. The carboxyl group, being either protected as an ester or not, is apparently sufficiently isolated from the remaining part of the DPA-Tyr moiety to influence the protonation processes of groups substantially involved in the luminescence emission.

UV-Vis studies of EuL^{1,2}. Further studies with the investigated complexes were performed by means of UV-Vis spectrophotometry, in order to reveal new insights that could not be obtained with the luminescence emission experiments.

Firstly, UV-Vis absorption spectra of solutions of **EuL^{1,2}** (50 μM) at pH 7.4 were recorded in the presence of various concentrations of Zn^{2+} (0–3 equiv). The spectra are dominated

© 2020 The Authors. Published by Wiley-VCH Verlag GmbH & Co. KGaA

by an intense absorption around 250 nm attributable to the pyridyl units of the DPA moiety,[23] and a second broad band with a maximum around 305 nm characteristic of the phenol group.[24] Addition of 1 equiv. of Zn^{2+} causes a slight blue shift of the band of **EuL^1** with maximum at 305 nm to 295 nm (Figure 5), whereas the same type of shift from 306 nm to 296 nm takes place for **EuL^2** (Figure S5 in the Supporting Information). Further addition of Zn^{2+} did not induce noticeable changes. This is consistent with the previously observed luminescence effects: binding of Zn^{2+} to the amine group of Tyr does not affect the UV spectrum of **EuL^1**, while **EuL^2** already exhibited insensitivity towards Zn^{2+} beyond 1 equiv. added (see above). Furthermore, the band with a maximum at 250 nm and 248 nm for **EuL^1** and **EuL^2**, respectively, experiences a dramatic intensity decrease upon Zn^{2+} addition, which confirms the binding of the metal ion to the DPA moiety of the ligand. No UV-Vis absorbance changes were found for **EuL^3** or **EuL^4** (50 μM) at pH 7.4 in the presence and absence of Zn^{2+}.

UV-Vis absorption of **EuL^1** (50 μM) was also studied at different pH values to find out whether the phenol group of tyrosine is involved in binding to Eu^{3+}. The absorption spectra were recorded from pH ~ 4.0 to ~11.0 (Figure 6). Increasing the pH provokes a decrease of the band at 303 nm while a new maximum at 335 nm develops. Conversely, the band at 250 nm remains nearly unaffected by pH. The analysis of the absorbance changes at 335 nm provides a $pK_a = 9.4 \pm 0.5$. These results

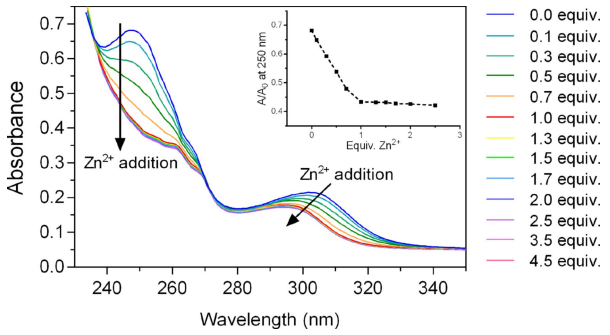

Figure 5. UV-Vis absorption titrations of **EuL^1** (50 μM) with Zn^{2+} (50 mM HEPES buffer at pH 7.4). Inset: absorption intensity variations at 250 nm with Zn^{2+} addition.

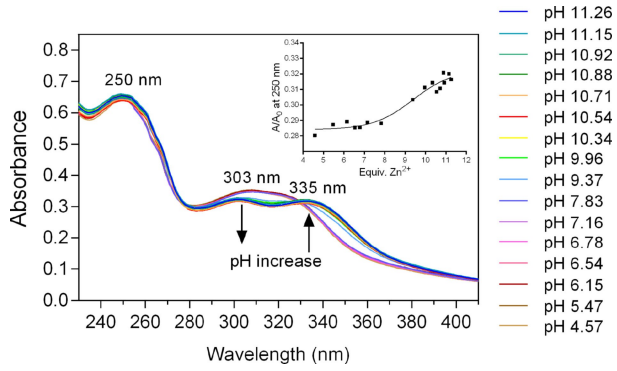

Figure 6. Changes in the UV-Vis absorbance of **EuL^1** (50 μM in water) upon variations in pH. Inset: absorption intensity variations at 335 nm with pH changes.

suggest that the phenol group is involved in protonation/deprotonation processes, specifically being protonated at physiological pH.

Finally, to confirm the binding relationship of Zn^{2+} with **EuL^{1,2}**, a method of continuous variation was applied on both complexes and Job's plots were obtained (Figure S6 in the Supporting Information).[25] The experiments were performed with the total concentration of $[Zn^{2+}] + [\mathbf{EuL^{1,2}}] = 50$ μM and their result confirmed that **EuL^1** possesses two Zn^{2+}-binding sites, as it presents a maximum close to $x_{Zn2+} = 0.60$.[26] The same experiment performed for **EuL^2** indicates a 1:1 ratio of binding to Zn^{2+}, matching the obtained results from the luminescence titration experiments (see above).

Longitudinal relaxivity of Gd^{3+} complexes

The coordination properties of the studied systems were also assessed by preparing highly paramagnetic Gd^{3+} analogues of **EuL^{1,2}** and testing their relaxometric response in the presence of Zn^{2+}. The synthesis of **GdL^{1,2}** was performed in the same manner as for **EuL^{1,2}** by chelating Gd^{3+} in the form of the chloride hydrate with the respective ligand **L^{1,2}**. Subsequently, the longitudinal relaxivity, r_1, was determined for both complexes in the absence or presence of different concentrations of Zn^{2+} (Figure S7 in the Supporting Information). Initial r_1 values for both complexes are high (7.35 and 7.95 $mM^{-1}s^{-1}$ for **GdL^1** and **GdL^2**, respectively), which suggests the presence of monohydrated complexes in both cases. Addition of Zn^{2+} to **GdL^1** causes a rather small increase in relaxivity of ~10% ($r_1 =$ 8.21 $mM^{-1}s^{-1}$ upon addition of 5 equiv. of Zn^{2+}). This small relaxivity enhancement is not compatible with a change in the hydration number of the complex, but rather to some effect on the rotational dynamics of the complex in the presence of two Zn^{2+} ions or a change in the water exchange. Additionally, the relaxometric titrations of **GdL^2** with Zn^{2+} resulted in negligible relaxivity changes, with the r_1 value remaining in the range 7.9–8.0 $mM^{-1}s^{-1}$, confirming that the hydration number of the complex remains unchanged when Zn^{2+} is added to the solution. Moreover, r_1 values for both complexes are very similar to those recorded under identical conditions for monohydrated GdDO3A-type derivatives with similar size.[27] This suggests that the phenolate group remains coordinated to the metal ion upon protonation, and that the electron withdrawing effect of the nitro substituent at position 4 of the phenol group in the complex reported by Woods et al. is responsible for its dissociation when protonated.[22]

DFT calculations

DFT calculations were carried out to aid the rationalization of the observed results. The optimized structure of the **EuL^1** complex supports octadentate binding of the ligand to the Eu^{3+} ion, with average Eu–N and Eu–$O_{carboxylate}$ distances of 2.67 and 2.38 Å, respectively. The Eu–O_{phenol} distance of 2.56 Å is relatively long, and decreases to 2.34 Å upon deprotonation.

© 2020 The Authors. Published by Wiley-VCH Verlag GmbH & Co. KGaA

Calculations were also performed on the **EuL^{1}ZnCl$_2$** system, in which two chloride anions were included to complete the square-pyramidal coordination of Zn^{2+} observed for DPA derivatives of this metal ion in the presence of Cl^-.[28] The experimental data were obtained using 100 mM KCl as background electrolyte, and thus Cl^- coordination is expected.

The coordination of Zn^{2+} to the DPA moiety provokes little changes in the Eu^{3+} coordination environment (Figure 7), but significant changes in the frontier molecular orbitals. Indeed, the HOMO of **EuL^1** is mainly located on the amine nitrogen atom of the DPA moiety, with some contribution of the lone pairs of the pyridyl nitrogen atoms. Conversely, the LUMO is comprised of π orbitals of the pyridyl and phenol groups. The HOMO of the **EuL^{1}ZnCl$_2$** system is predicted to be centered on one of the carboxylate groups of the DO3A unit, while the main contributions to the LUMO are provided by π orbitals of the pyridyl groups. Both the HOMO and the LUMO are significantly stabilized upon Zn^{2+} coordination (Figure 7). These results are in line with a PET mechanism being responsible for the turn-on luminescence response of **EuL^1** to Zn^{2+}.[9b] PET sensors are responsive electron donor-acceptor probes in which the HOMO of the donor (the lone pair of the amine N atoms in this case) presents a higher energy than the acceptor in the absence of the target analyte. As a result, excitation of the LUMO results in an electron transfer from the HOMO of the donor to the HOMO of the acceptor, quenching the emission of the probe. Coordination of Zn^{2+} to the DPA moiety reduces the energy of the HOMO of the donor, enhancing the overall luminescence.

Conclusion

We studied a series of EuDO3A-based complexes as potential luminescence chemosensors for the detection of Zn^{2+}. All complexes were appended with tyrosine as a chromophore, while only two that contained DPA as a recognition moiety for Zn^{2+} exhibited properties suitable for the desired luminescent sensors. In the absence of Zn^{2+}, only weak luminescence of each probe was observed due to quenching of luminescence caused by the PET mechanism involving the deprotonated amine group of DPA. Upon the addition of Zn^{2+}, both DPA-containing probes displayed large increases in Eu^{3+}-centered luminescent emission, which reached up to sevenfold enhancement. The ion selectivity experiments demonstrated the specificity of these probes toward Zn^{2+} over other biologically relevant metal ions. The two complexes without a DPA-moiety did not show any obvious luminescent enhancement for any of the studied metal ions, emphasizing the essential role of DPA for the recognition of Zn^{2+}. Extensive luminescence, UV-Vis and relaxometric studies that involved pH and Zn^{2+} titrations or theoretical DFT calculations revealed the major properties of the chemosensors in aqueous solution. They also provided essential mechanistic insights of their interaction with Zn^{2+} and the consequence of this interaction on the subsequent luminescence emission. For future studies, it would be desirable to design a complex in which both protonation constants (of the amine of DPA and phenol on Tyr units) are lowered, thus promoting greater change in the luminescence intensity upon Zn^{2+} addition by: a) achieving greater quenching by the DPA group/free electron pair in the absence of Zn^{2+}, and b) further enhancing the signal by deprotonating the phenol group upon Zn^{2+} addition. Overall, the results reported in this work allowed for precise quantitative analysis of the interaction of Eu^{3+} luminescent complexes together with Zn^{2+} as the target analyte. It also provided important insights which can assist further in establishing Ln^{3+}-based complexes as useful chemosensors for potential biological applications that range from the development of different bioassays to medical optical imaging.

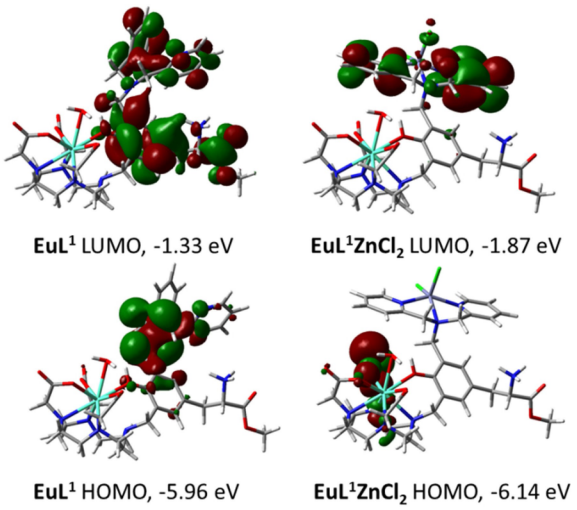

Figure 7. Views of the frontier molecular orbitals of **EuL^1** and **EuL^{1}ZnCl$_2$** obtained with DFT calculations.

Experimental Section

General

The reagents were purchased from Aldrich and were used without further purification. Compound **1** was synthesised following a previously published procedure.[13] Purification of synthesized compounds was performed using silica gel 60 (0.03–0.2 mm) from Carl Roth (Germany). The buffer solution (0.1 M HEPES, pH 7.4) was prepared by dissolving solid HEPES in HPLC grade water. After the solution became clear, aqueous NaOH (1 M) was added to adjust the pH to the desired value. The buffer solution was used without degassing. All UV-vis absorption and fluorescence spectra were recorded on an Agilent Cary 60 UV-Vis Spectrophotometer and a QuantaMaster™ 3 PH fluorescence spectrometer from Photon Technology International, Inc. (USA), respectively. Low resolution mass spectra were recorded on an ion trap SL 1100 system Agilent with an electrospray ionization source. High resolution mass spectra were recorded on a Bruker Daltonics APEX II (FT-ICR-MS) with an electrospray ionization source. MALDI-TOF-MS analysis was performed by The Scripps Center for Mass Spectrometry, La Jolla, CA. ^{1}H and ^{13}C NMR spectra were recorded on a Bruker Avance III 300 MHz spectrometer at 25 °C. Processing was performed using TopSpin 2.1 (Bruker GmbH) and ACD/SpecManager 9.0 (Advanced Chemistry Development, Inc.). The concentration of Gd^{3+} and Eu^{3+}

© 2020 The Authors. Published by Wiley-VCH Verlag GmbH & Co. KGaA

in analyzed solutions was determined using the bulk magnetic susceptibility shift (BMS).[29]

Synthetic procedures

3-[3-[(Bis-pyridin-2-ylmethyl-amino)-methyl]-4-hydroxy-5-(4,7,10-tris-*tert*-butoxycarbonylmethyl-1,4,7,10 tetraaza-cyclododec-1-ylmethyl)-phenyl]-2-*tert*-butoxycarbonylamino-propionic acid methyl ester (2): DO3A-*t*Bu (1.544 g, 3.00 mmol) and paraformaldehyde (0.198 g, 6.6 mmol) in 10 mL toluene were stirred at 60 °C until the solution became clear. Then, compound **1** (3.040 g, 6.00 mmol) was added to the reaction mixture and a few drops of DBU were added shortly afterwards, followed by stirring for 6 h at 110 °C. Upon reaction completion, the reaction mixture was evaporated and purified by silica gel column chromatography using DCM/MeOH (v/v, 20:1) as the eluent, affording 1.333 g (43%) of compound **2** as a light yellow oil. **^{1}H NMR** ($CDCl_3$, 300MHz): δ (ppm): 1.40, 1.42 (s, 36H, CCH_3); 2.22–3.49 (br, 24H, NCH_2); 3.69 (s, 3H, OCH_3); 3.81 (s, 6H, NCH_2C); 4.39–4.58 (m, 1H, NHC*H*); 6.83–6.96 (m, 2H, phOH); 7.09–8.72 (m, 8H, pyridyl). **^{13}C NMR** ($CDCl_3$, 75MHz): δ (ppm): 27.8, 28.1 (12C, CCH_3); 37.3 (1C, phCH_2CH); 51.4, 51.6, 51.7, 51.9, 52.6, 52.7 (8C, NCH_2CH_2); 53.5 (1C, OCH_3); 55.6, 56.1 (3C, NCH_2CO); 54.7 (2C, phCH_2N); 57.3 (1C, NH_2C*H*); 60.1 (2C, pyCH_2); 80.5, 82.2 (4C, *C*CH_3); 121.7, 122.7 (4C, *C*CHCH, NCH*C*H); 123.2, 125.2 (2C, HOC*C*H); 128.7 (2C, *C*CHC); 129.9 (1C, CH*C*CH); 136.3 (2C, CCH*C*H); 148.8 (2C, NCH*C*H); 149.1 (1C, OH*C*); 155.7 (1C, NHCO*C*); 160.0 (2C, NCCH); 170.8, 171.1, 172.5 (4C, *C*O). ESI-TOF/MS: (*m/z*) $[M+H]^+$ calcd. for $C_{55}H_{85}N_8O_{11}^+$: 1033.6332; found: 1033.6325.

2-Amino-3-[3-[(bis-pyridin-2-ylmethyl-amino)-methyl]-4-hydroxy-5-(4,7,10-tris-carboxymethyl-1,4,7,10 tetraaza-cyclododec-1-ylmethyl)-phenyl]-propionic acid methyl ester (L^1): Compound **2** (1.033 g, 1.00 mmol) was dissolved in 5 mL TFA/DCM (v/v 50/50) and the solution was stirred at room temperature overnight. After purification by HPLC, pure H_3L^1 (0.604 g, 79%) was obtained. **^{1}H NMR** (D_2O, 300MHz): δ (ppm): 2.81–3.49 (br, 24H, NCH_2); 3.67 (s, 8H, NCH_2Ar); 3.73 (s, 3H, OCH_3); 4.26–4.42 (m, 1H, NH_2C*H*); 6.77, 7.31 (s, 2H, ph); 7.19 (d, $J=7.2$ Hz, 2H, NCHC*H*); 7.21 (d, $J=7.0$ Hz, 2H, NCC*H*); 7.63 (t, $J=7.7$ Hz, 2H, CHCHC*H*); 8.32 (d, $J=4.5$ Hz, 2H, NC*H*CH). **^{13}C NMR** (D_2O, 75MHz): δ (ppm): 34.6 (1C, phCH_2CH); 48.5–50.7 (8C, NCH_2CH_2); 53.4 (1C, OCH_3); 53.6 (1C, NH_2CH); 55.6, 56.3, 56.8 (3C, NCH_2CO); 55.9 (2C„ phCH_2N); 59.3 (2C, pyCH_2); 123.3, 123.6 (4C, CCHCH); 124.4, 126.4 (2C, HOCCH); 130.8 (1C, CHCCH); 132.4 (2C, CCHC); 138.2 (2C, CCHCH); 148.2 (2C, NCCH); 154.0 (1C, OHC); 156.0 (2C, NCHCH); 170.7 (4C, *C*O). ESI-TOF/MS: (*m/z*) $[M-H]^-$ calcd. for $C_{38}H_{51}N_8O_9^-$: 763.3785; found: 763.3785.

2-Amino-3-[3-[(bis-pyridin-2-ylmethyl-amino)-methyl]-4-hydroxy-5-(4,7,10-tris-carboxymethyl-1,4,7,10 tetraaza-cyclododec-1-ylmethyl)-phenyl]-propionic acid (L^2): Compound L^1 (0.306 g, 0.40 mmol) was dissolved in 5 mL methanol and LiOH was added. Then the mixture was stirred at room temperature overnight. After filtering, the methanol was evaporated. The crude mixture was dissolved in water and the pH was adjusted to 7. The mixture was then purified by HPLC to yield 0.222 g (74%) of H_3L^2 as a light yellow powder. **^{1}H NMR** (D_2O, 300MHz): δ (ppm): 2.61–3.49 (br, 24H, NCH_2); 3.53–3.87 (br, 8H, NCH_2Ar); 3.95–4.05 (m, 1H, NH_2C*H*); 6.83, 6.96 (s, 2H, phOH); 7.02–7.39 (m, 4H, NCHC*H*, NCC*H*); 7.64 (t, $J=$ 7.3 Hz, 2H, CHCHC*H*); 8.24 (d, $J=4.3$ Hz, 2H, NC*H*CH). **^{13}C NMR** (D_2O, 75MHz): δ (ppm): 34.8 (1C, phCH_2CH); 47.7, 50.7 (8C, NCH_2CH_2); 52.6 (1C, NH_2C*H*); 53.4, 54.5 (3C, NCH_2CO); 56.7 (2C, phCH_2N); 58.7 (2C, pyCH_2); 126.4, 127.5 (4C, CCHCH); 127.9 (2C, HOCCH); 134.3 (2C, CCHC); 134.8 (1C, CHCCH); 141.5 (2C, CCHCH); 146.5 (2C, NCCH); 151.9 (2C, NCHCH); 152.7 (1C, OHC); 163.0, 162.6 (2C, NCCH); 173.3 (4C, *C*O). ESI-TOF/MS: (*m/z*) $[M-H]^-$ calcd. for $C_{37}H_{49}N_8O_9^-$: 749.3628; found: 749.3631.

2-*tert*-Butoxycarbonylamino-3-[4-hydroxy-3-(4,7,10-tris-*tert*-butoxycarbonylmethyl-1,4,7,10 tetraazacyclododec-1-ylmethyl)-phenyl]-propionic acid methyl ester (3): DO3A-*t*Bu (1.029 g, 2.00 mmol) and paraformaldehyde (0.132 g, 4.40 mmol) were stirred in 5 mL toluene at 65 °C until the solution became clear. Then, Boc-Tyrosine-OMe (1.299 g, 4.40 mmol) was added to the reaction mixture and a few drops of DBU were added shortly afterwards, followed by stirring for 3 h at 65 °C. Upon reaction completion, the reaction mixture was evaporated and purified by silica gel column chromatography using DCM/MeOH (v/v, 20:1) as the eluent to yield 1.217 g (74%) of **3** as light yellow oil. **^{1}H NMR** ($CDCl_3$, 300MHz): δ (ppm): 1.01–1.17 (br, 36H, CCH_3), 1.79–2.78 (br, 26H, NCH_2), 3.35 (s, 3H, OCH_3), 4.65 (m, 1H, NHC*H*), 6.47 (d, $J=7.9$ Hz, 1H, HOC=C*H*), 6.61 (s, 1H, C=C*H*=C); 6.85–7.00 (m, 1H, C=CH=C*H*). **^{13}C NMR** ($CDCl_3$, 75MHz): δ (ppm): 27.8, 28.1 (12C, CH_2CH_3); 36.9 (1C, phCH_2); 46.3 (1C, OCH_3); 49.5, 49.6 (8C, NCH_2CH_2); 51.9 (1C, phCH_2N); 53.7, 55.2, 55.8 (3C, NCH_2CO); 54.6 (1C, $NHCH_2$); 79.5, 82.0, 82.1, (4C, $C(CH_3)_3$); 117.9, 123.7, 126.7, 129.3, 132.7 (5C, ph); 154.3 (1C, OH*C*); 154.7 (1C, NH*C*O); 171.9 (3C, CH_2CO); 172.4 (1C, CH*C*O). ESI-TOF/MS: (*m/z*) $[M+H]^+$ calcd. for $C_{42}H_{72}N_5O_{11}^+$: 822.5223, found: 822.5225.

2-Amino-3-[4-hydroxy-3-(4,7,10-tris-carboxymethyl-1,4,7,10 tetraaza-cyclododec-1-ylmethyl)-phenyl]-propionic acid methyl ester (L^3): Compound **3** (1.200 g, 1.46 mmol) was dissolved in 6 mL TFA/DCM (v/v 50/50) and the solution was stirred at room temperature overnight. Pure H_3L^3 (0.671 g, 83%) was obtained by HPLC. **^{1}H NMR** (D_2O, 300MHz): δ (ppm): 2.99–3.49 (br, 24H, NCH_2, phCH_2CH), 3.58 (s, 3H, OCH_3), 3.94 (s, 2H, phCH_2N), 3.98–4.13 (m, 1H, NH_2C*H*), 6.78–6.93 (br, 1H, C=CH=C*H*), 7.12 (d, 1H, $J=6.6$ Hz, HOC=C*H*), 7.21 (s, 1H, C=C*H*=CH). **^{13}C NMR** (D_2O, 75MHz): δ (ppm): 34.7 (1C, phCH_2); 46.7 (1C, OCH_3); 47.8 (1C, NH_2C*H*); 51.6 (1C, phCH_2N); 52.1, 53.5, 54.1, 54.5 (8C, NCH_2CH_2); 55.5 (3C, NCH_2CO); 116.13, 126.1, 133.2, 133.5 (5C, ph); 154.7 (1C, OH*C*); 169.3, 169.9 (3C, CH_2CO); 173.6 (1C, CH*C*O). ESI-TOF/MS: (*m/z*) $[M-H]^-$ calcd. for $C_{25}H_{38}N_5O_9^-$ *m/z* 552.2675; found: 552.2677.

2-Amino-3-[4-hydroxy-3-(4,7,10-tris-carboxymethyl-1,4,7,10 tetraaza-cyclododec-1-ylmethyl)-phenyl]-propionic acid (L^4): Compound L^3 (0.277 g, 0.50 mmol) was dissolved in 5 mL methanol and LiOH was added. Then the mixture was stirred at room temperature overnight. After filtering, methanol was evaporated. The crude mixture was dissolved in water and the pH was adjusted to 7. Then the mixture was purified by HPLC to yield 0.129 g (71%) of H_3L^4 as a white powder. **^{1}H NMR** (D_2O, 300MHz): δ (ppm): 2.80–3.39 (br, 24H, NCH_2, phCH_2CH), 3.72 (s, 2H, phCH_2N), 4.22–4.42 (m, 1H, NH_2C*H*), 6.65–6.85 (br, 2H, C=CH=C*H*), 6.95–7.11 (br, 1H, HOC=C*H*), 7.13–7.30 (m, 1H, C=C*H*=CH). **^{13}C NMR** (D_2O, 75MHz): δ (ppm): 34.6, 35.2, 35.7 (1C, phCH_2CH); 53.5, 53.8 (1C, phCH_2N); 55.0, 55.2 (8C, NCH_2CH_2); 55.5, 55.7 (3C, NCH_2CO); 56.5, 56.6 (1C, NH_2CH); 116.7, 126.1, 127.1, 128.1, 131.5, 131.9, 133.2 (5C, ph); 153.9, 154.1 (1C, OH*C*); 170.4, 172.8, 173.8 (4C, *C*O). ESI-TOF/MS: (*m/z*) $[M-H]^-$ calcd. for $C_{24}H_{36}N_5O_9^-$: 538.2519; found: 538.2519.

General procedure for the preparation of the Eu^{3+} and Gd^{3+} complexes: The introduction of the europium (for L^{1-4}) or gadolinium (for L^{1-2}) ions into the macrocyclic framework was carried out at pH ~7.0 adjusted by 0.1 M NaOH solution. To a stirred aqueous solution of ligand, a solution of $EuCl_3\cdot6H_2O$ or $GdCl_3\cdot6H_2O$ was prepared in water and was added dropwise to the ligand solution in 1:1 molar ratios. The reaction mixture was heated to 50 °C and stirred overnight. The pH of the solution was periodically adjusted to 7.0 by addition of 0.1 M NaOH solution. The reaction mixture was then cooled to room temperature. The yellow solid compound was obtained by lyophilization. The formation of the metal complexes EuL^{1-4} was confirmed by mass spectrometry.

EuL^1: ESI-LRMS: (*m/z*) $[M+H]^+$ calcd. for $C_{38}H_{50}EuN_8O_9^+$: 915.3; found: 915.3.

© 2020 The Authors. Published by Wiley-VCH Verlag GmbH & Co. KGaA

GdL^1: ESI-LRMS: (*m/z*) $[M-H]^-$ calcd. for $C_{38}H_{48}GdN_8O_9^-$: 918.3; found: 918.3.

EuL^2: ESI-LRMS: (*m/z*) $[M-H]^-$ calcd. for $C_{37}H_{46}EuN_8O_9^-$: 899.3; found: 899.3.

GdL^2: ESI-LRMS: (*m/z*) $[M-H]^-$ calcd. for $C_{37}H_{46}GdN_8O_9^-$: 904.3; found: 904.3.

EuL^3: ESI-LRMS: (*m/z*) $[M+H]^+$ calcd. for $C_{25}H_{37}EuN_5O_9^+$: 704.2; found: 704.2.

EuL^4: ESI-LRMS: (*m/z*) $[M-H]^-$ calcd. for $C_{24}H_{33}EuN_5O_9^-$: 688.1; found: 688.1.

UV/Vis spectroscopy: UV-Vis spectra of complexes **EuL$^{1-4}$** (50 μM) in 50 mM HEPES buffer at pH 7.4 were obtained at 25 °C on a Cary Varian double beam spectrophotometer (Cary). The pH effect on absorptions of **EuL^1** (50 μM) was studied with changes of pH values from 4.57 to 11.26. Zn^{2+}-sensitive absorptions of **EuL^{1,2}** were studied with the addition of various concentrations of Zn^{2+} (0–3 mM).

Luminescence studies: The Zn^{2+}-sensitive luminescence spectra of 50 μM complex in 50 mM HEPES buffer at pH 7.4 were measured at 25 °C (excitation at 322 nm), with the addition of various concentrations of Zn^{2+} (0–4.0 equiv. of Zn^{2+}). The pH effect on luminescence of **EuL^{1,2}** and **EuL^{1,2}Zn** was studied with changes of pH values from 4 to 12, respectively. The pK_a values were fitted by a Boltzmann-type sigmoid.[30] Association constants were determined by analysing the emission spectra in the range 560–720 nm with the HYPERQUAD 2008 (HypSpec) program.[31]

Zn^{2+}-binding titrations: All the Zn^{2+}-binding titrations were measured in 50 mM HEPES buffer at pH 7.4 at 25 °C. The total molar concentration of complex and Zn^{2+} was 50 μM.

Metal ion selectivity: For metal ion selectivity experiments, stock solutions (0.05 M) of NaCl, KCl, $CaCl_2$, $MgCl_2$, $FeCl_2$, $FeCl_3$, $CuCl_2$ and $ZnCl_2$ were prepared. The appropriate concentrations (50 μM) of Eu^{3+} complex were prepared by the dilution method using HPLC grade water and HEPES buffer. All data were recorded in HEPES buffer (50 mM, pH 7.4); excitation wavelength at 322 nm; slit widths were 1 nm for both excitation and emission.

Relaxometric Titrations: Proton longitudinal relaxometric titrations with Zn^{2+} were performed at 7.0 T, 25 °C, and pH 7.4 (50 mM HEPES buffer) using inversion recovery (T_1) pulse sequences. A $ZnCl_2$ solution of known concentration was added stepwise to the **GdL$^{1-2}$** solution (starting concentration 3.0 mM Gd^{3+}), and measurements of T_1 were performed after each addition of the analyte. The longitudinal relaxivities, r_1, were calculated from Eq. 1 where $T_{1,obs}$ is the measured T_1, T_{1d} is the diamagnetic contribution of the solvent, and [Gd] is the actual Gd^{3+} concentration at each point of the titration.

$$1/T_{1,obs} = T_{1d} + r_1 \times [Gd] \quad (1)$$

DFT calculations: Geometry optimizations and analytical frequency calculations of the **EuL^1** and **EuL^{1}ZnCl$_2$** systems were carried out using the Gaussian 09 program package.[32] The frequency analysis confirmed that the optimized geometries corresponded to local energy minima in all cases. In these calculations we used the hybrid meta generalized gradient approximation (hybrid meta-GGA) with the TPSSh exchange-correlation functional.[33] Relativistic effects were considered using the large-core effective core potential of Dolg et al.[34] for Eu, in combination with the associated (7s6p5d)/[5s4p3d] GTO valence basis. The 6-31G(d,p) basis set was used for all other atoms. The TPSSh functional in combination with the large-core approximation was found to provide good results in studies focusing on the structures and energetics of lanthanide complexes.[35] The quality of the integration grid was increased from the default values using the integral = ultrafine keyword in Gaussian 09.

Acknowledgements

The financial supports of the China Scholarship Council (PhD fellowship to Gaoji Wang) and the German Research Foundation (DFG, grant AN 716/7-1) for this research are acknowledged. C.P.-I. acknowledges the support of Centro de Supercomputación de Galicia (CESGA).

Keywords: lanthanides · luminescence · photoinduced electron transfer · tyrosine · zinc

[1] a) K. Hanaoka, K. Kikuchi, H. Kojima, Y. Urano, T. Nagano, *J. Am. Chem. Soc.* **2004**, *126*, 12470–12476; b) W. Maret, Y. Li, *Chem. Rev.* **2009**, *109*, 4682–4707; c) C. S. Bonnet, *Coord. Chem. Rev.* **2018**, *369*, 91–104; d) K. P. Carter, A. M. Young, A. E. Palmer, *Chem. Rev.* **2014**, *114*, 4564–4601; e) P. N. Basa, S. Antala, R. E. Dempski, S. C. Burdette, *Angew. Chem. Int. Ed.* **2015**, *54*, 13027–13031.
[2] L. De Leon-Rodriguez, A. J. M. Lubag, A. D. Sherry, *Inorg. Chim. Acta* **2012**, *393*, 12–23.
[3] D. J. Eide, *Metallomics* **2011**, *3*, 1124–1129.
[4] a) P. J. Jiang, Z. J. Guo, *Coord. Chem. Rev.* **2004**, *248*, 205–229; b) K. Kikuchi, K. Komatsu, T. Nagano, *Curr. Opin. Chem. Biol.* **2004**, *8*, 182–191; c) T. Gunnlaugsson, T. C. Lee, R. Parkesh, *Org. Biomol. Chem.* **2003**, *1*, 3265–3267; d) G. J. Stasiuk, F. Minuzzi, M. Sae-Heng, C. Rivas, H. P. Juretschke, L. Piemonti, P. R. Allegrini, D. Laurent, A. R. Duckworth, A. Beeby, G. A. Rutter, N. J. Long, *Chem. Eur. J.* **2015**, *21*, 5023–5033.
[5] a) S. Biniecki, S. Kabzinska, *Ann. Pharm. Fr.* **1964**, *22*, 685–687; b) J. R. Johnson, H. Jiang, B. D. Smith, *Bioconjugate Chem.* **2008**, *19*, 1033–1039.
[6] a) E. R. Milaeva, D. B. Shpakovsky, Y. A. Gracheva, S. I. Orlova, V. V. Maduar, B. N. Tarasevich, N. N. Meleshonkova, L. G. Dubova, E. F. Shevtsova, *Dalton Trans.* **2013**, *42*, 6817–6828; b) E. J. O'Neil, H. Jiang, B. D. Smith, *Supramol. Chem.* **2013**, *25*, 315–322; c) B. Roy, A. S. Rao, K. H. Ahn, *Org. Biomol. Chem.* **2011**, *9*, 7774–7779; d) S. A. Yoon, J. Lee, M. H. Lee, *Sens. Actuators B* **2018**, *258*, 50–55.
[7] B. A. Wong, S. Friedle, S. J. Lippard, *J. Am. Chem. Soc.* **2009**, *131*, 7142–7152.
[8] a) J. Fan, X. Peng, Y. Wu, E. Lu, J. Hou, H. Zhang, R. Zhang, X. Fu, *J. Lumin.* **2005**, *114*, 125–130; b) A. P. de Silva, T. S. Moody, G. D. Wright, *Analyst* **2009**, *134*, 2385–2393; c) M. J. Culzoni, A. M. de la Pena, A. Machuca, H. C. Goicoechea, R. Brasca, R. Babiano, *Talanta* **2013**, *117*, 288–296; d) D. Escudero, *Acc. Chem. Res.* **2016**, *49*, 1816–1824.
[9] a) H. Akiba, J. Sumaoka, M. Komiyama, *Chem. Eur. J.* **2010**, *16*, 5018–5025; b) M. Roger, M. Regueiro-Figueroa, C. Ben Azzeddine, V. Patinec, C. S. Bonnet, C. Platas-Iglesias, R. Tripier, *Eur. J. Inorg. Chem.* **2014**, *2014*, 1072–1081; c) O. Reany, T. Gunnlaugsson, D. Parker, *J. Chem. Soc. Perkin Trans. 2* **2000**, 1819–1831; d) K. Hanaoka, K. Kikuchi, H. Kojima, Y. Urano, T. Nagano, *Angew. Chem. Int. Ed.* **2003**, *42*, 2996–2999; e) M. L. Aulsebrook, B. Graham, M. R. Grace, K. L. Tuck, *Tetrahedron* **2014**, *70*, 4367–4372.
[10] a) S. J. A. Pope, R. H. Laye, *Dalton Trans.* **2006**, 3108–3113; b) S. Shuvaev, M. Starck, D. Parker, *Chem. Eur. J.* **2017**, *23*, 9974–9989.
[11] S. Shuvaev, M. A. Fox, D. Parker, *Angew. Chem. Int. Ed.* **2018**, *57*, 7488–7492.
[12] a) L. H. Fornander, B. B. Feng, T. Beke-Somfai, B. Norden, *J. Phys. Chem. B* **2014**, *118*, 9247–9257; b) J. M. Antosiewicz, D. Shugar, *Biophys. Rev. Lett.* **2016**, *8*, 151–161.
[13] R. G. Hanshaw, E. J. O'Neil, M. Foley, R. T. Carpenter, B. D. Smith, *J. Mater. Chem.* **2005**, *15*, 2707–2713.
[14] W. C. Shieh, S. Dell, O. Repic, *Org. Lett.* **2001**, *3*, 4279–4281.
[15] K. Binnemans, *Coord. Chem. Rev.* **2015**, *295*, 1–45.
[16] V. Hlinova, A. Jaros, T. David, I. Cisarova, J. Kotek, V. Kubicek, P. Hermann, *New J. Chem.* **2018**, *42*, 7713–7722.

© 2020 The Authors. Published by Wiley-VCH Verlag GmbH & Co. KGaA

[17] L. Fabbrizzi, M. Licchelli, P. Pallavicini, *Acc. Chem. Res.* **1999**, *32*, 846–853.
[18] S. W. Zhang, R. Adhikari, M. X. Fang, N. Dorh, C. Li, M. Jaishi, J. T. Zhang, A. Tiwari, R. Pati, F. T. Luo, H. Y. Liu, *ACS Sens.* **2016**, *1*, 1408–1415.
[19] G. K. Walkup, S. C. Burdette, S. J. Lippard, R. Y. Tsien, *J. Am. Chem. Soc.* **2000**, *122*, 5644–5645.
[20] N. Q. Jie, J. H. Yang, X. R. Huang, W. Y. Ma, *Anal. Proc.* **1995**, *32*, 427–429.
[21] B. Daly, J. Ling, A. P. de Silva, *Chem. Soc. Rev.* **2015**, *44*, 4203–4211.
[22] M. Woods, G. E. Kiefer, S. Bott, A. Castillo-Muzquiz, C. Eshelbrenner, L. Michaudet, K. McMillan, S. D. K. Mudigunda, D. Grin, G. Tircso, S. R. Zhang, P. Zhao, A. D. Sherry, *J. Am. Chem. Soc.* **2004**, *126*, 9248–9256.
[23] I. Carreira-Barral, T. Rodriguez-Blas, C. Platas-Iglesias, A. de Bias, D. Esteban-Gomez, *Inorg. Chem.* **2014**, *53*, 2554–2568.
[24] O. A. Blackburn, M. Tropiano, L. S. Natrajan, A. M. Kenwright, S. Faulkner, *Chem. Commun.* **2016**, *52*, 6111–6114.
[25] W. Likussar, D. F. Boltz, *Anal. Chem.* **1971**, *43*, 1265–1272.
[26] J. S. Renny, L. L. Tomasevich, E. H. Tallmadge, D. B. Collum, *Angew. Chem. Int. Ed.* **2013**, *52*, 11998–12013.
[27] M. Regueiro-Figueroa, S. Gündüz, V. Patinec, N. K. Logothetis, D. Esteban-Gómez, R. Tripier, G. Angelovski, C. Platas-Iglesias, *Inorg. Chem.* **2015**, *54*, 10342–10350.
[28] a) Y. P. Zhang, Z. Y. Ma, C. Y. Gao, X. Qiao, J. L. Tian, W. Gu, X. Liu, J. Y. Xu, J. Z. Zhao, S. P. Yan, *New J. Chem.* **2016**, *40*, 7513–7521; b) Y. I. Kim, Y. S. Lee, H. J. Seo, J. Y. Lee, S. K. Kang, *Acta Crystallogr. Sect. E* **2007**, *63*, M2810-U1669.
[29] D. M. Corsi, C. Platas-Iglesias, H. van Bekkum, J. A. Peters, *Magn. Reson. Chem.* **2001**, *39*, 723–726.
[30] J. Aguiar, P. Carpena, J. A. Molina-Bolivar, C. C. Ruiz, *J. Colloid Interface Sci.* **2003**, *258*, 116–122.
[31] P. Gans, A. Sabatini, A. Vacca, *Talanta* **1996**, *43*, 1739–1753.
[32] M. J. Frisch, G. W. Trucks, H. B. Schlegel, G. E. Scuseria, M. A. Robb, J. R. Cheeseman, G. Scalmani, V. Barone, B. Mennucci, G. A. Petersson, H. Nakatsuji, M. Caricato, X. Li, H. P. Hratchian, A. F. Izmaylov, J. Bloino, G. Zheng, J. L. Sonnenberg, M. Hada, M. Ehara, K. Toyota, R. Fukuda, J. Hasegawa, M. Ishida, T. Nakajima, Y. Honda, O. Kitao, H. Nakai, T. Vreven, J. A. Montgomery, J. E. Peralta, F. Ogliaro, M. Bearpark, J. J. Heyd, E. Brothers, K. N. Kudin, V. N. Staroverov, R. Kobayashi, J. Normand, K. Raghavachari, A. Rendell, J. C. Burant, S. S. Iyengar, J. Tomasi, M. Cossi, N. Rega, J. M. Millam, M. Klene, J. E. Knox, J. B. Cross, V. Bakken, C. Adamo, J. Jaramillo, R. Gomperts, R. E. Stratmann, O. Yazyev, A. J. Austin, R. Cammi, C. Pomelli, J. W. Ochterski, R. L. Martin, K. Morokuma, V. G. Zakrzewski, G. A. Voth, P. Salvador, J. J. Dannenberg, S. Dapprich, A. D. Daniels, Farkas, J. B. Foresman, J. V. Ortiz, J. Cioslowski, D. J. Fox in *Gaussian 09, Revision B.01*, *Vol.* Gaussian, Inc., Wallingford CT, **2009**.
[33] J. M. Tao, J. P. Perdew, V. N. Staroverov, G. E. Scuseria, *Phys. Rev. Lett.* **2003**, *91*, 146401.
[34] M. Dolg, H. Stoll, A. Savin, H. Preuss, *Theor. Chim. Acta* **1989**, *75*, 173–194.
[35] a) M. Regueiro-Figueroa, D. Esteban-Gómez, A. de Blas, T. Rodríguez-Blas, C. Platas-Iglesias, *Chem. Eur. J.* **2014**, *20*, 3974–3981; b) M. Regueiro-Figueroa, C. Platas-Iglesias, *J. Phys. Chem. A* **2015**, *119*, 6436–6445.

Manuscript received: December 13, 2019
Revised manuscript received: January 8, 2020

© 2020 The Authors. Published by Wiley-VCH Verlag GmbH & Co. KGaA